Available online at www.sciencedirect.com
ScienceDirect
Journal of Nuclear Materials 375 (2008) 8–25
journal of nuclear materials
www.elsevier.com/locate/jnucmat

Oxygen stoichiometry shift of irradiated LWR-fuels at high burn-ups: Review of data and alternative interpretation of recently published results

J. Spino [a,*], P. Peerani [b]

[a] European Commission, Joint Research Centre, Institute for Transuranium Elements, P.O. Box 2340, D-76125 Karlsruhe, Germany
[b] European Commission, Joint Research Centre, Institute for the Protection and Security of the Citizen, I-21020 Ispra, Italy

Received 30 May 2007; accepted 26 October 2007

Abstract

The available oxygen potential data of LWR-fuels by the EFM-method have been reviewed and compared with thermodynamic data of equivalent simulated fuels and mixed oxide systems, combined with the analysis of lattice parameter data. Up to burn-ups of 70–80 GWd/tM the comparison confirmed traditional predictions anticipating the fuels to remain quasi stoichiometric along irradiation. However, recent predictions of a fuel with average burn-up around 100 GWd/tM becoming definitely hypostoichiometric were not confirmed. At average burn-ups around 80 GWd/tM and above, it is shown that the fuels tend to acquire progressively slightly hyperstoichiometric O/M ratios. The maximum derived O/M ratio for an average burn-up of 100 GWd/tM lies around 2.001 and 2.002. Though slight, the stoichiometry shift may have a measurable accelerating impact on fission gas diffusion and release.

1. Introduction

The fission of uranium and plutonium atoms in uranium dioxide-based nuclear fuels is to be seen as an oxidative process. This is because the generated fission products, though appearing in a number twice as larger as the destroyed fissile atoms cannot bind completely the oxygen atoms liberated during fission (roughly: two atoms per fission event). Indeed, not all fission products are able to bind oxygen (typical case of Kr and Xe). On the other hand, the main elements forming oxides (i.e., Zr, Y, the rare earths (RE), Sr and Ba) exhibit an average valence that is lower than that of the actinides in the fuel and bind comparatively less oxygen. In addition, other fission products that potentially oxidise remain in practice as pure metal or as precipitate-alloy, because the free energy of formation of their oxides is much higher than the oxygen potential available in the fuel (case of the noble metal atoms).

Whether a given fission product element oxidises in the reactor is dictated by the oxygen potential of the oxide in equilibrium with the metal ($\Delta GO_2 = \mathrm{RTln}\, pO_2$; $pO_2 =$ oxygen partial pressure), which in the thermodynamic standard state is related to the free energy of formation of the oxide (ΔG_f^o) and the ratio of the stoichiometry coefficients of the reaction. The element will thus oxidise only if the oxygen potential of the fuel equals or exceeds that of the corresponding metal/metal-oxide mixture. The master diagram governing these situations as a function of temperature is shown in Fig. 1. In the illustrated case the isopleths (i.e., the oxygen potential vs. T curves) of the phase $U_{0.6}Pu_{0.4}O_{2\pm x}$ (as from Ref. [1]) are used to represent those of the fuel at high burn-ups. The justification for this assumption is given in Section 2.

From Fig. 1 it is seen that for a stoichiometric or slightly hypostoichiometric fuel the critical boundary delimiting the elements prevented from oxidation is represented by Cs and Rb at temperatures around and below 1000 K, and by Mo at higher temperatures. In this situation the major elements becoming oxidised are Zr, Y + RE, Sr

* Corresponding author. Tel.: +49 7247 951 233; fax: +49 7247 951 590.
E-mail address: Jose-Luis.Spino@ec.europa.eu (J. Spino).

0022-3115/$ - see front matter © 2007 Elsevier B.V. All rights reserved.
doi:10.1016/j.jnucmat.2007.10.007

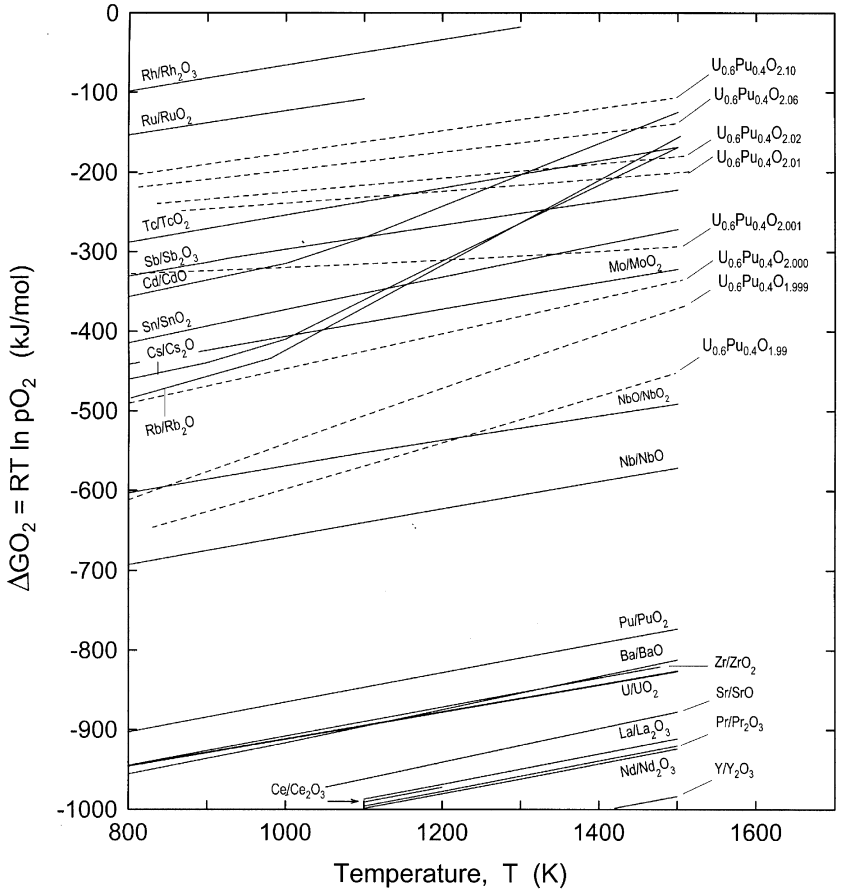

Fig. 1. Equilibrium oxygen potentials of different metal/metal-oxide mixtures and of the system $U_{0.6}Pu_{0.4}O_{2\pm x}$ in the temperature range 800–1500 K. Data sources: Refs. [1–9].

and Ba, which for a thermal-reactor-fuel with 10%-burn-up can bind only 15.6 of the 20 oxygen atoms liberated every 10 fissions (details provided in Section 4). The unbound oxygen contributes first to elevate the O/M ratio of the fuel and then to oxidise the available molybdenum. Further oxidation of the fuel and/or of other fission products becomes only possible after completion or eventual stagnation of the oxidation of Mo. The mixture Mo/MoO_2 buffers so far the oxygen potential of the whole system. This description is obviously not new. It was first provided by O'Boyle and co-workers [2] and by Holleck and Kleykamp [3], almost four decades ago. Works by Davies and Etwart [4] and by Findlay [5] and a similar description by Olander [6] followed, all of them emphasizing the oxidative role of burn-up in oxide fuels. We remark that the only difference between the present Fig. 1 and similar figures of Refs. [2,3,6] is the update of the ΔGO_2-data, which was here undertaken according to Refs. [1–9].

The former statements apply only under consideration of a closed fuel-fission products system. If the cladding is included as a reactive component of the system the described O/M increase of the fuel with burn-up appears delayed or eventually neutralised, because of the oxygen-getter action of the cladding. Kleykamp described this situation for both stainless-steel-canned FBR-fuels [9] and Zr-alloy-canned LWR-fuels [10]. For the latter case he demonstrated that the oxygen uptake at the inner face of the cladding was equivalent to a fuel oxidation of 0.006 O/U units at a burn-up of 4.3 at.%. This coincided with a previous estimation of a stoichiometry shift of the fuel of $\Delta(O/M) = +0.0013$ per% burn-up [10]. On the base of the measured Mo-concentration in the metallic precipitates, the fuel itself was predicted by Kleykamp [10] to remain roughly stoichiometric, or eventually slightly hypostoichiometric, over the whole radius.

Coinciding with the above predictions, hitherto oxygen potential determinations by the galvanic method (EMF) on various irradiated PWR and BWR fuels in the burn-up range 11–75 GWd/tM [11–14] showed that the investigated fuels, with different degrees of inner cladding oxidation, remained approximately stoichiometric (or slightly hypostoichiometric, e.g. $O/M \cong 1.997$–1.999 [11–14]) upon irradiation. However, opposing to Refs. [11–14], in a recent work by Walker et al. [15] where the ΔGO_2-values of a LWR-fuel with ≈100 GWd/tM burn-up were also determined by the EMF-method at different radial positions, quite low O/M values were assigned to the fuel (depending on the conditions, between 1.94 and 1.97), notwithstanding

the measured ΔGO_2 values were much higher than those previously reported in Refs. [11–14] at equivalent temperatures, especially in the outer parts of the fuel [15].

In view of this discrepancy and because of the decisive influence of the oxygen stoichiometry of the fuel in basic processes such as diffusion, creep, gas release, thermal conductivity and others, it is the aim of this work to re-analyse the whole set of ΔGO_2 data available on LWR-fuels [11–15], to visualize the trend of the O/M variation towards high burn-ups mainly by comparison with existent thermodynamic information. As a complement, oxygen balance calculations will be shown emphasizing the role of Mo in the fuel oxidation, as also a detailed analysis of the variation of the lattice constant of UO_2 with different parameters (solute content, oxygen potential, radiation damage) will be given in support of the deduced trends. Due to their impact in the oxygen balance, the compositional data of metallic and oxide precipitates in irradiated and simulated fuels as a function of the oxygen potential will be reviewed. Finally, a short analysis of the implications of the results in the fuel behaviour, as well as a scope of possible necessary corroborating measurements will be provided.

2. Comparison of measured ΔGO_2 data of irradiated and simulated fuels

Undoubtedly the most complete and most widely used method for measuring the molar quantities (ΔGO_2) of non-volatile oxides as a function of temperature and composition is thermogravimetry (TG). By this method the sample is equilibrated at a given temperature with an atmosphere of known oxygen potential (pO_2). Under the premise that the sample interchanges only oxygen atoms with the atmosphere, the corresponding oxygen stoichiometry in the solid is determined by weight variation, using given points of the phase diagram of the oxide as reference. In that way, sets of values (ΔGO_2, O/M, T) are obtained at equilibrium. By contrast, the alternative galvanic method (EMF) can only provide sets of values (ΔGO_2, T) as the sample is equilibrated with a buffer Me/MeO mixture; the corresponding O/M values must be gained separately. In the case of pure and doped UO_2, the TG and the EMF-methods have been shown to yield congruent results. Just some examples in this sense are the EMF-measurements by Saito [16] in UO_{2+x} and the dual EMF- and TG-measurements by Une and Oguma [17,18] in (U, Gd)$O_{2\pm x}$. As routine, for the EFM-tests, the oxygen stoichiometry of the sample is checked either by the gravimetric method [16] or/and by the spectrophotometric method (U^{6+}/U^{4+} ratio) [18,19].

In the case of irradiated fuels, thermogravimetric determinations of the O/M ratio are impracticable because of spurious weight changes caused by release of volatile components, and because of the lack of information of the actual phase boundaries of the oxide, which serve as reference for the oxidation state (for UO_2, typically the borders at O/M = 2 or O/M = 2.667). Also, determinations of the oxygen stoichiometry via chemical methods (e.g. spectrophotometry, coulometry) in spent LWR-fuels had been up to now rare, with only two known cases in the open literature at burn-ups of 2.5 [20] and 34 GWd/tM [21]. For this reason, a reasonable way to estimate the oxygen stoichiometry of the irradiated fuel remains the comparison of the measured oxygen potential, e.g. by the EFM-method, with 'ΔGO_2 vs. O/M'-data of chemically similar systems, i.e., simulated fuels. However, although the thermodynamic data for UO_{2+x} and the ternary oxides $U_{1-y}Pu_yO_{2\pm x}$, $U_{1-y}Ce_yO_{2\pm x}$ and $U_{1-z}La_zO_{2\pm x}$ (La = Y, La, Nd, Gd) is relatively extensive [22–28], the experimental data of simulated fuels is restricted to one work by Une and Oguma on LWR-fuels [29] and one by Woodley on MOX-fuels [30], both up to 10 at.% burn-up.

Because of the above reasons, in this work only the TG-ΔGO_2 measurements by Une and Oguma [29] on simulated LWR-fuels at 1273 K, and for the sake of completion those by Woodley [30] on simulated MOX-fuels at the same temperature are used to compare with the measured EMF-ΔGO_2 values as a function of the O/M ratio and burn-up. For the analysis of the temperature dependence, the comparison is performed with the isopleths 'ΔGO_2 vs. T' of the system $U_{0.6}Pu_{0.4}O_{2\pm x}$(O/M as parameter), the thermochemical data of which has been comprehensively compiled by Lindemer and co-workers [1,25,26]. Although not typical of LWR-fuels but more applicable to fresh Fast Breeder or LWR–MOX-fuels, this mixed oxide system with 40% dissolved Pu-atoms in the UO_2 lattice exhibits both in the hyperstoichiometric and the hypostoichiometric range ΔGO_2-values that circumscribe most of the data measured for simulated LWR and MOX-fuels with up to 10 at.% burn-up [29,30] (see Fig. 2 in Section 2.1, upper envelope curve (marks: stars)). The system is thus taken as conservative upper bound for the ΔGO_2-values of irradiated LWR-fuels, limiting in excess the expected increase of the oxygen potential of UO_2 during burn-up (at a given O/M ratio) by substitution of U by fission products- and Pu-atoms.

2.1. Oxygen potential vs. O/M ratio

In Fig. 2 (left hand side) the available oxygen potential data at 1273 K for UO_2 and simulated LWR- and MOX-25% Pu-fuels with burn-ups up to 10 at.% are plotted as a function of the O/M ratio. For comparison, the measured data for the reference system $U_{0.75}Pu_{0.25}O_{2-x}$ [30] and compiled data by Lindemer et al. [25–27] for the system $U_{0.6}Pu_{0.4}O_{2\pm x}$ are also included. Though belonging to different oxides, the hypostoichiometric and hyperstoichiometric branches of the data in Fig. 2 define the typical s-shaped behaviour of the 'ΔGO_2 vs. O/M' curves of uranium dioxide-based systems around O/M = 2, with a jump of almost 200 kJ/mol (i.e., more than eight orders of magnitude difference in the corresponding oxygen partial pressure) between the slight hypostoichiometric and the slight hyperstoichiometric ranges, which denote in general the difficulty to reduce these oxides below

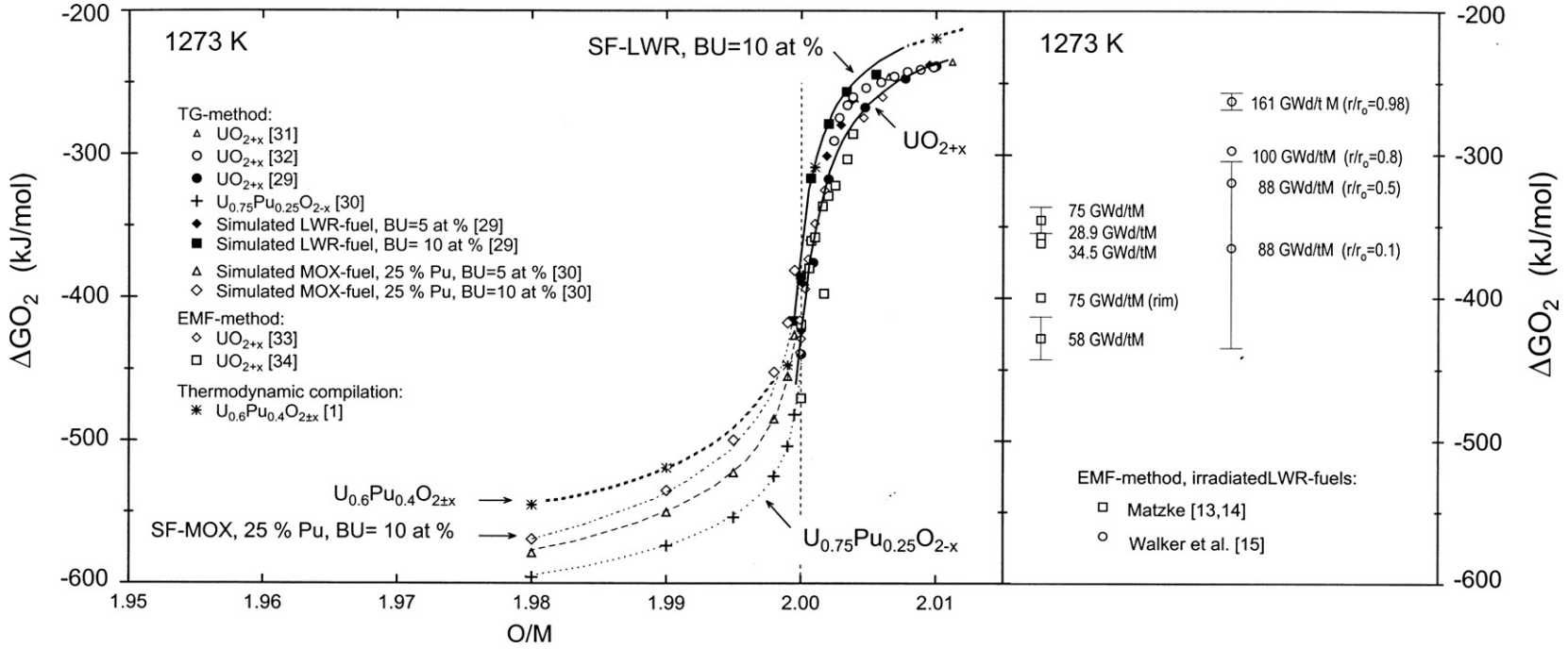

Fig. 2. Compilation of oxygen potential vs. oxygen to metal ratios data for the systems UO_{2+x} [29,31–34], $U_{0.75}Pu_{0.25}O_{2-x}$ [30], simulated LWR-fuels (Burn-up = 5, 10 at.%) [29] and simulated MOX-fuels (Pu = 0.25; burn-up = 5, 10 at.%) [30], according to thermogravimetric (TG) and galvanic-solid electrolyte (EMF) measurements from different sources, and thermodynamic calculations for the system $U_{0.6}Pu_{0.4}O_{2\pm x}$ [1]. Comparison with oxygen potential measurements by the EMF-method of irradiated fuels in the burn-up range 28.9–100 GWd/tM [13–15].

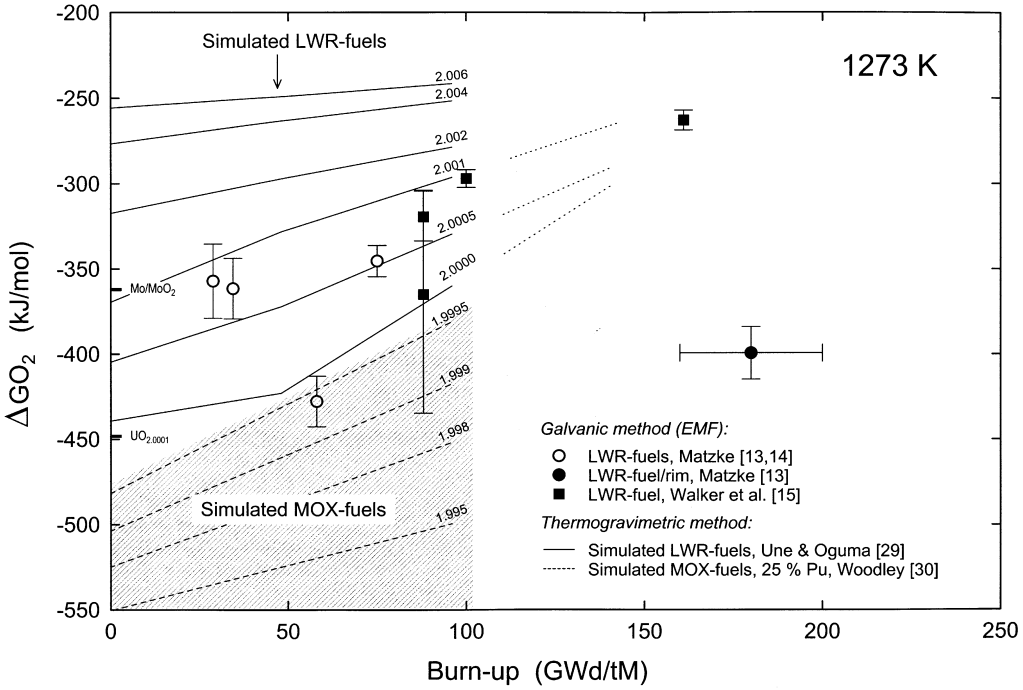

Fig. 3. Compilation of oxygen potential vs. burn-up data from thermogravimetric measurements of simulated LWR [29] and MOX [30] fuels. Comparison with oxygen potential data measured by the EMF-method for irradiated fuels with average burn-ups in the range 28.9–100 GWd/tM [13–15].

O/M = 2. In the case of pure UO_2, due to the literal inexistence of the substoichiometric phase at temperatures below ~1500 K [24], the ΔGO_2 vs. O/M isotherms are to be assumed only valid for O/M $\geqslant$ 2. The data composing this isotherm at 1273 K, i.e., as from the early measurements by Gerdanian and Dodé [31] and Thomas et al. [32] (TG-method) and by Markin and Bones [33] (EMF-method), and more recent measurements by Baranov and Godin [34] (EMF-method) and Une and Oguma [29] (TG-method), show some scatter for O/M > 2.0025 (see discussion of this scatter in the recent review of [24]) (Fig. 2). For lower O/M ratios the data agree satisfactorily; the nominal stoichiometry for UO_2 at 1273 K is thus shown to be reached at oxygen potentials around −480 kJ/mol (Fig. 2) [24].

As evident from Fig. 2 the effect of adding Pu and/or fission products (lanthanides) to UO_2 is first of all to open the hypostoichiometric range of the mixed oxide. The second effect is to elevate the equilibrium oxygen potential at constant O/M ratio, i.e., in other words, to reduce the oxygen stoichiometry at constant ΔGO_2. This effect is more marked in the hypostoichiometric range and increases as the Pu and/or fission products concentrations increase (Fig. 2, left hand side). As a result, for a LWR-fuel with a burn-up of about 10 at.% and at a temperature of 1273 K, the nominal fuel stoichiometry (O/M = 2) is to be reached at a ΔGO_2 value of around −400 kJ/mol, i.e., about 80 kJ/mol above that of stoichiometric UO_2 (Fig. 2, left hand side).

On the right hand side of Fig. 2 the available measured ΔGO_2 data for irradiated LWR-fuels with average burn-ups between ~29 GWd/tM and 100 GWd/tM and at a temperature of 1273 K are plotted with their respective error bands as given by the corresponding authors [13–15]. Walker et al.'s data [15] are labelled according to the originally quoted local burn-ups (pellet radial position are given between parentheses). Differently, Matzke's data [13,14] are labelled according to the original fuel average burn-ups. As the majority of these samples corresponded to pellet central positions, both average and local burn-ups would fairly coincide. Only in the case of the rim sample of the fuel with 75 GWd/tM [13], a range of local burn-ups between 160 and 200 GWd/tM is to be assigned. This corresponds to the scatter of values given in the original work [13]. Comparison of the two sides of Fig. 2 indicate that except for the rim sample of the fuel with 75 GWd/tM and the pellet-centre sample of the fuel with 58 GWd/tM burn-up from Matzke's data [13,14], which appear to be stoichiometric or hypostoichiometric, all other fuels lie in the hyperstoichiometric range, with O/M ratios ranging between approximately 2.001 and 2.002 (Fig. 2).

2.2. Oxygen potential vs. burn-up

In Fig. 3 the measured ΔGO_2 data for simulated LWR-fuels [29] (and simulated MOX-fuels [30]) and irradiated LWR-fuels [13–15] are plotted as a function of burn-up for the temperature of 1273 K, with the error bands as given in the original literature sources. For comparison, also the oxygen potential of the mixture Mo/MoO_2 as from Fig. 1 and that of $UO_{2.001}$ as from the chemical-thermodynamic

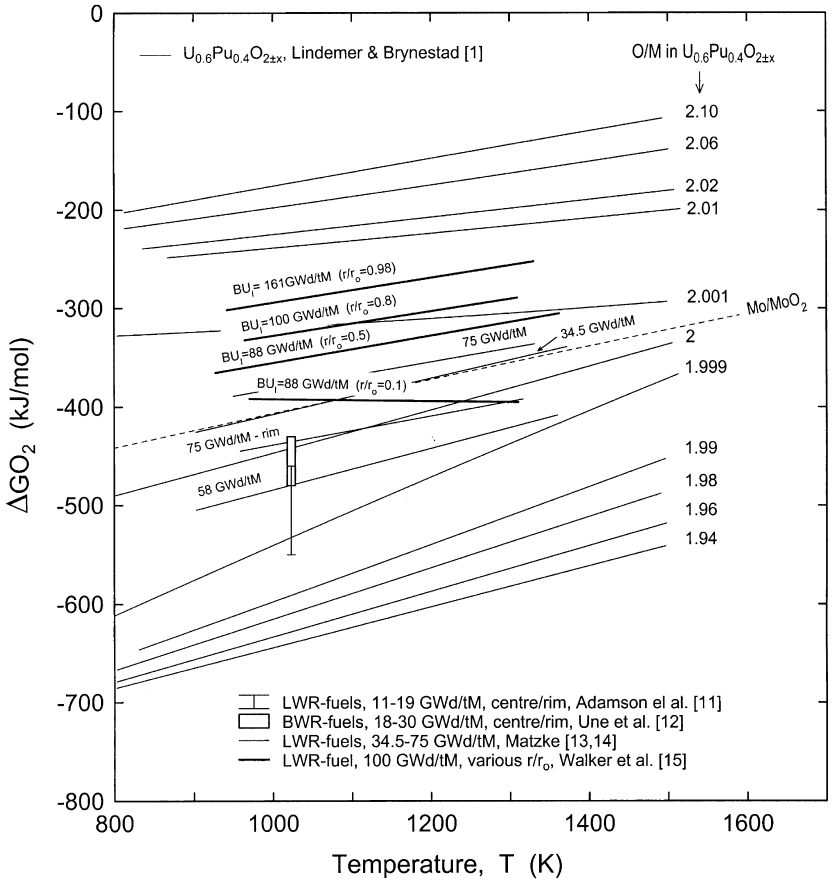

Fig. 4. Oxygen potential vs. temperature data in the range 800–1500 K for the system $U_{0.6}Pu_{0.4}O_{2\pm x}$ according thermodynamic assessment by Lindemer and Brynestad [1]. Comparison with oxygen potential data measured by the EMF-method for irradiated fuels with average burn-ups in the range 11–100 GWd/tM [11–15].

model of Lindemer and Besmann [22] are given in the figure. For the simulated LWR-fuels, the values of the isopleths at O/M = 2, 2.0005, 2.001 were interpolated from the scanned original 'ΔGO_2 vs. O/M' curves as given in Fig. 2a of Ref. [29]. For the other isopleths at O/M = 2.002, 2.004 and 2.006, the values were taken from the original 'ΔGO_2 vs. burn-up' curves as given in Fig. 3a of Ref. [29]. For the simulated MOX-fuels, the values were taken from the similar Fig. 4 of Ref. [30].

In line with the suggestions of the former section, the comparison of the measured ΔGO_2 values for simulated and irradiated fuels as a function of burn-up indicate all irradiated fuels having a stoichiometric or slightly hyperstoichiometric oxygen composition (O/M comprised between 2 and 2.001), except for the already mentioned fuel with 58 GWd/tM average burn-up and the rim sample of the fuel with 75 GWd/tM average burn-up as from Matzke's data [13,14], which appear to be slightly hypostoichiometric (Fig. 3). The last referred rim sample falls remarkably out of the general trend of the measurements (Fig. 3). Eventually, a contribution in this sample of the ZrO_2-based interaction layer with the cladding is conceivable, which would have made the oxygen potential to drop excessively.

2.3. Oxygen potential vs. temperature

Corroboration of the trends mentioned in the two previous sections is provided in Fig. 4 of this section where the measured ΔGO_2 values of the different irradiated LWR-fuels are plotted as a function of temperature. In addition to the fuels analysed in the previous sections, here also the low burn-up data by Adamson et al. [11] and Une et al. [12] at the temperature of 1023 K are included. The data are compared with the isopleths of the system $U_{0.6}Pu_{0.4}O_{2\pm x}$ at different O/M ratios as compiled by Lindemer and Brynestad [1], which, as mentioned previously, are taken as conservative limit for the oxygen potential of irradiated LWR-fuels with up at least 10 at.% burn-up (Section 2).

Comparison of the measured and calculated data in Fig. 4 confirm that for all temperatures examined, say between 950 and 1350 K, the majority of the fuels investigated were in the stoichiometric or the slightly hypostoichiometric range. To the last category belong the already mentioned fuel with 58 GWd/tM average burn-up and the rim sample of the fuel with 75 GWd/tM average burn-up (for $T > 1100$ K), as from Matzke's data [13,14], and the low burn-up fuels examined by Adamson et al.

[11] and Une et al. [12]. However, the O/M ratio in all of them was potentially never inferior to 1.999 (Fig. 4). On the other hand, the fuel samples with the largest burn-ups, i.e., at and above 88 GWd/tM, as from Walker's et al. data [15], show a clear trend to steadily increase the oxygen stoichiometry on increasing the local burn-up, decidedly surpassing the O/M ratio mark of 2.001 for burn-ups higher than 100 GWd/tM (Fig. 4). This opposes the conclusions of the authors in Ref. [15], which attributed these fuels as being definitely hypostoichiometric. Further evidences supplied in following sections reinforce the contrary hypothesis defended in the present work that the considered high burn-up fuels exhibited an oxygen surplus.

3. Partition of Mo between metallic and oxide precipitates as a function of the oxygen potential

Since for the reasons given in the introduction the oxidation of the fission product Mo appears to control the oxygen potential of the fuel, the concentration of Mo in the segregated metallic and oxide phases in the fuel have been used traditionally to monitor the oxygen potential of the system (the solubility of Mo in the UO_2 matrix is considered negligible). The EPMA-works by Kleykamp and co-workers in irradiated fuels [35,36] and the careful out-of-pile phase studies by Paschoal et al. [37–39] have been an icon in this area, setting the range of compositions of the metal–alloy (Mo, Tc, Ru, Rh, Pd) and oxide (Perovskite-type) precipitates in the fuel, known, respectively, as 'white' and 'grey' phase inclusions. Via the equilibrium

$$[\mathrm{Mo}]_{\mathrm{alloy}} + (\mathrm{O}_2) = [\mathrm{MoO}_2]_{\mathrm{Perovskite}} \tag{1}$$

the oxygen potential of the system was calculated via the expression

$$\Delta G\mathrm{O}_2 = \Delta G_{\mathrm{f}}^{\mathrm{o}}\langle \mathrm{MoO}_2\rangle + RT\ln(x\mathrm{MoO}_2 \cdot \gamma\mathrm{MoO}_2 / x\mathrm{Mo} \cdot \gamma\mathrm{Mo}) \tag{2}$$

where $\Delta G_{\mathrm{f}}^{\mathrm{o}}\langle \mathrm{MoO}_2\rangle$ is the free energy of formation of molybdenum dioxide, and $x\mathrm{MoO}_2$ and $x\mathrm{Mo}$ are the molar fractions of MoO_2 in the Perovskite phase and of Mo in the metal–alloy precipitates, and $\gamma\mathrm{MoO}_2$ and $\gamma\mathrm{Mo}$ the respective activity coefficients [35,36], often taken as unity [40]. By virtue of (2), due to the high content of Mo verified in the metallic precipitates, it was concluded that the oxygen potential of the fuel remained around that corresponding to the exact fuel stoichiometry along almost the whole fuel radius ($\Delta G\mathrm{O}_2 \approx -400$ kJ/mol, $T \approx 1000$–2000 K, O/M ≈ 2), up to burn-ups of 4.3 at.% [10]. The oxygen excess accumulated during irradiation (values given in the introduction) was assumed to be consumed in the internal oxidation of the cladding [10].

However, one of the most intriguing facts concerning the partition of Mo between metallic and oxide precipitates in the fuel is the persistence of quite large fractions of this element in the metallic precipitates up to very high oxygen potentials, under conditions which cannot be represented by (2). Indeed, as shown in Refs. [40,41] for simulated fuels with up to 30 at.% burn-up, molar fraction of 20–30% of Mo can be found in the metallic precipitates after equilibration of the fuel, e.g. at 1673 K at an oxygen potential as high as −170 kJ/mol, which is, in principle, incompatible with Eq. (2). These observations also contradict previous thermochemical calculations for LWR-fuels, indicating for these oxygen potentials the main fraction of Mo to be most likely present in oxide form (as molybdate), rather than as metal [42].

Studies of Ref. [40] at temperatures of 1673 K demonstrate that the lattice parameters (a, c) of the metallic precipitates in the fuel (hexagonal ε-phase), both proportional to the Mo-concentration in the alloy [37], sharply decrease for oxygen potentials around that of the Mo/MoO_2 equilibrium (∼−300 kJ/mol) and rapidly stagnate after exceeding this value, showing saturating a-values of 0.274–0.275 nm, which according to Paschoal [37] indicate Mo-concentrations of the order of 20–25 at.% in the alloy. In parallel with this, the authors of Ref. [40] demonstrated also that at the same temperature the lattice parameter of the oxide precipitates in the fuel (grey phase, cubic-Perovskite), which according to [37] varies inversely proportional to the molar concentration of $BaMoO_3$ in this phase, continuously decreased on increasing the oxygen potential and stagnated after the latter approached a value of ∼−250 kJ/mol, indicating a saturating content of $BaMoO_3$ in the grey phase of ∼45 mol%, in agreement with [37]. For higher oxygen potentials, Ref. [40] shows that the cubic-Perovskite phase changed to the tetragonal phase of the Scheelite-type ($BaMoO_4$), which has been shown to coexist in equilibrium with metallic Mo [37].

Despite the fact that Refs. [37–41] refer to studies with non-irradiated samples simulating the fuel and precipitate phases, their results suggest that under irradiation the possibility may exist that large portions of non-oxidised Mo could be retained at high oxygen potentials, in coexistence with oxide precipitates of the Scheelite-type ($BaMoO_4$). For illustration of the above, Figs. 5 and 6 show the pseudoternary equilibrium diagrams of the systems representing the metallic and oxide precipitates in LWR-fuels as per Refs. [37–39], as well as the compositions determined for both types of precipitates in irradiated [9,36–39,43,44] and simulated fuels [40,41,45], the latter for various oxygen potentials. Fig. 5 shows that the minimum Mo-concentration found in the alloy precipitates under all conditions was of the order of 15 at.%; the average of all measured Mo-fractions in these precipitates reaches about 35 at.% (Fig. 5).

4. Estimation of the O/M ratio from fuel composition calculations

In the formerly cited work of Ref. [15] an estimation of the O/M ratio for an irradiated LWR-fuel with average burn-up 100 GWd/tM was performed following the method of Davies and Edwart [4]. For this calculation,

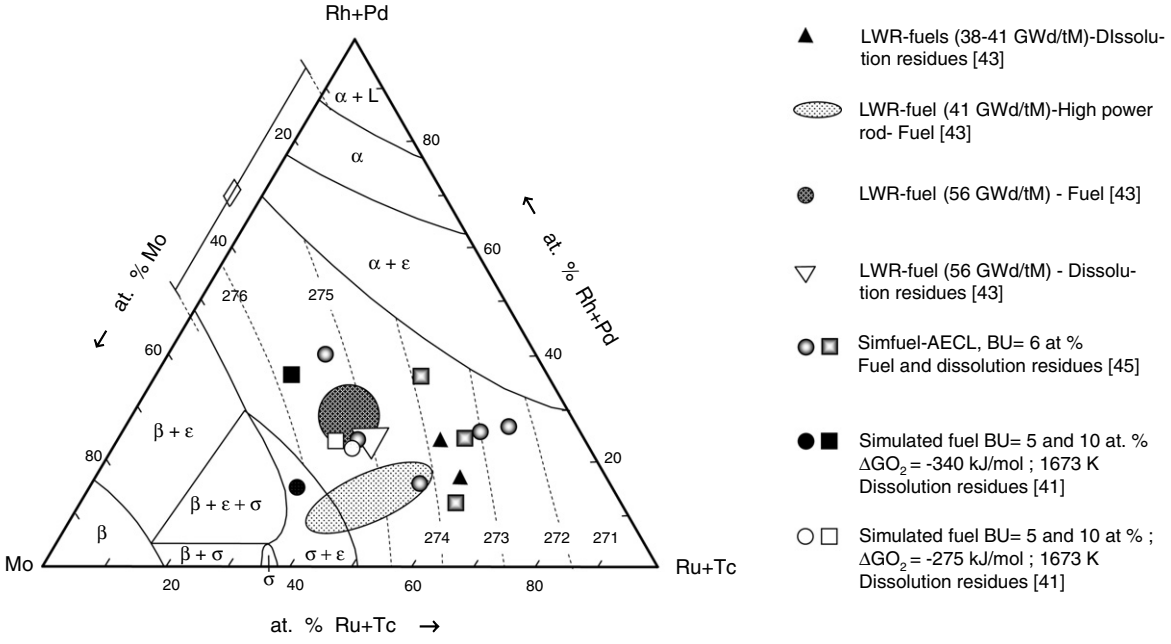

Fig. 5. Isothermal section of the pseudoternary system Mo–Ru–$Rh_{0.5}Pd_{0.5}$ within the quaternary system Mo–Ru–Rh–Pd at 1700 °C and corresponding lattice constant curves of the hexagonal ε-phase (dotted lines: *a* in pm) according to Paschoal et al. [38]. Superimposition of measured compositions of metallic precipitates in irradiated [43] and simulated LWR-fuels [41,45]; the last after annealing of the fuels at two different the oxygen potential [41].

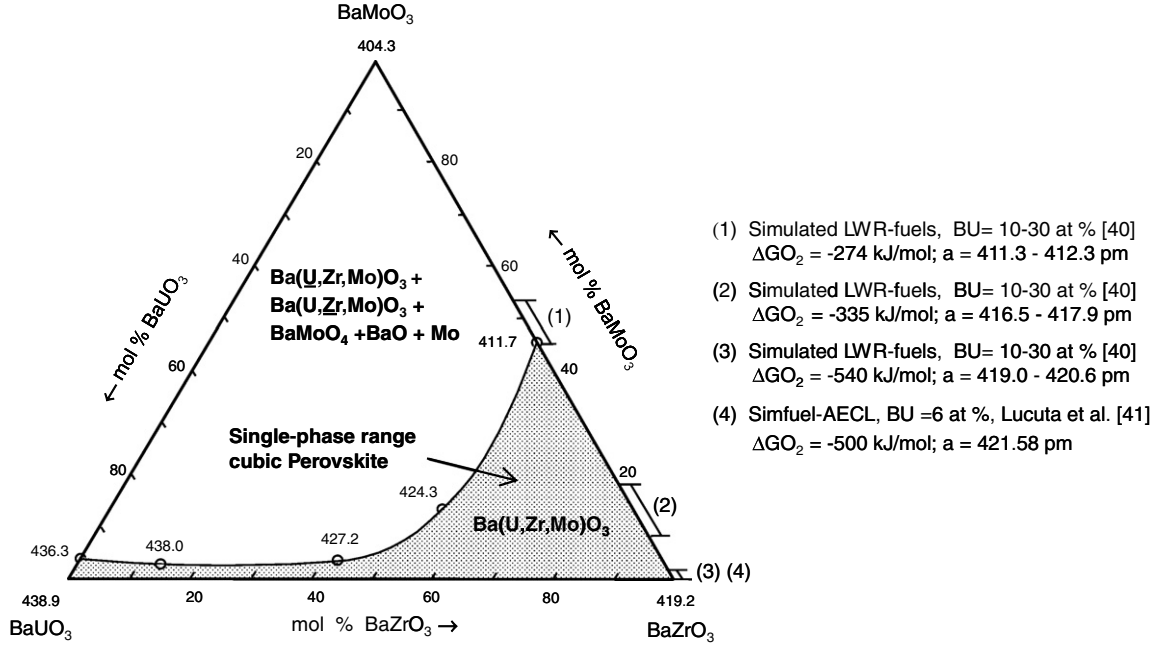

Fig. 6. Isothermal section of the pseudoternary $BaUO_3$–$BaZrO_3$–$BaMoO_3$ system at 1700 °C and lattice parameter *a* in pm according to Paschoal et al. [39]. Superimposition of composition and lattice constant ranges of ceramic precipitates as found in simulated fuels after annealing at different oxygen potentials [40,41].

the average composition of the fuel was used, as measured by ICP-MS after dissolution in 4 M HNO_3 acid. The concentrations of Pu and the fission products (Mo, Tc, Ru, Rh, Pd) were corrected for the amounts of these elements found in the residue of the dissolution [15]. Assumptions in [15] were that Sr and Zr fully dissolved in the fuel matrix; although previous works have shown that Sr and Zr form part primarily of the 'grey phase' precipitates, with maximum dissolved amounts of these elements in the fuel of, respectively, 12 and 25 mol% [36–39,46]. On the other hand, it was assumed in [15] that Mo and Cs were fully oxidised. The first of these two last assumptions is in discrepancy with previous works that show that not insignificant amounts of Mo remain in the fuel in metallic form even

Table 1
Actinides and fission products yields in a LWR-fuel with average burn-up 97.7 GWd/tM, as calculated with the code SCALE [47]

Element	Atomic weight	Weight concentration (g/ton initial HM atom)	Atomic concentration (% of initial HM-atom)
Heavy metal atoms			
U	238.00	8.84E+05	8.84E+01
Np	237.00	1.02E+03	1.02E−01
Pu	240.00	1.31E+04	1.30E+00
Am	242.00	1.69E+03	1.66E−01
Cm	244.00	9.14E+02	8.91E−02
Cf	249.00	2.74E−02	2.62E−06
Fission products			
Li	6.94	8.17E−02	2.80E−04
Be	9.01	4.31E−04	1.14E−06
C	12.01	7.57E−05	1.50E−07
Zn	65.37	3.64E−05	1.32E−08
Ga	69.72	3.13E−04	1.07E−07
Ge	72.59	9.37E−01	3.07E−04
As	74.92	2.80E−01	8.89E−05
Se	78.96	1.36E+02	4.08E−02
Rb	85.47	7.62E+02	2.12E−01
Sr	87.62	1.61E+03	4.38E−01
Y	88.91	9.79E+02	2.62E−01
Zr	91.22	8.45E+03	2.20E+00
Nb	92.91	8.41E−03	2.15E−06
Mo	95.94	9.25E+03	2.29E+00
Tc	97.00	1.74E+03	4.27E−01
Ru	101.07	7.69E+03	1.81E+00
Rh	102.91	7.48E+02	1.73E−01
Pd	106.40	6.89E+03	1.54E+00
Pd	106.40	6.89E+03	1.54E+00
Ag	107.87	2.78E+02	6.13E−02
Cd	112.40	7.41E+02	1.57E−01
In	114.84	2.50E+00	5.19E−04
Sn	118.69	1.94E+02	3.89E−02
Sb	121.75	2.79E+01	5.45E−03
Te	127.60	1.42E+03	2.64E−01
Ba	137.34	5.81E+03	1.01E+00
La	138.91	3.26E+03	5.58E−01
Ce	140.12	6.79E+03	1.15E+00
Pr	140.91	2.95E+03	4.98E−01
Nd	144.24	1.11E+04	1.84E+00
Pm	145.00	1.84E+01	3.02E−03
Sm	150.40	2.01E+03	3.19E−01
Eu	151.96	3.95E+02	6.18E−02
Gd	157.25	1.19E+03	1.80E−01
Dy	162.50	1.51E+01	2.21E−03
Tb	158.92	9.40E+00	1.41E−03
Ho	164.93	1.67E+00	2.40E−04
Er	167.26	1.03E+00	1.46E−04
Tm	168.93	1.44E−05	2.03E−09
Yb	173.04	3.49E−05	4.80E−09
Pb	207.19	9.23E−04	1.06E−07
Ra	226.00	2.61E−06	2.75E−10
Pa	231.04	6.60E−04	6.80E−08
Th	232.04	6.21E−03	6.37E−07
Gaseous and volatile fission products			
H	1.00	8.16E−02	1.94E−03
He	4.00	1.44E+01	8.56E−02
Br	79.09	4.86E+01	1.46E−02
Kr	83.80	8.01E+02	2.27E−01
I	126.90	6.64E+02	1.24E−01
Xe	131.29	1.59E+04	2.88E+00
Cs	132.91	6.34E+03	1.13E+00
Total atoms			1.12E+02

Table 2
Concentrations of actinides and selected fission products in a LWR-fuel with average burn-up 97.7 GWd/tM as from Table 1

Element	Concentration (% of initial HM atom)		Valence	Oxide formed		$\Delta G O_2$-threshold for element oxidation at 1273 K[c] (kJ/mol)	Equivalent O/M ratio in $U_{0.6}Pu_{0.4}O_{2\pm x}$ at 1273 K[c]
	Present work	Ref. [15]		$(U, Me)O_{2\pm x}$	Separate oxide		
Actinides	90.000	90.940	4	x		−840 to −880	≪1.99
Zr	2.200	2.590	4	x[b]	x	−860	≪1.99
Y + RE	4.880	5.650	4[a]	x		−960 to −1030	≪1.99
Sr	0.440	0.510	2, 4[a]	x[b]	x	−930	≪1.99
Ba	1.010	0.830	2		x	−860	≪1.99
Mo	2.290	0.920	4		x	−362	2.0003
Sn	0.040		4		x	−318	2.0008
Cs	1.130	1.240	1		x	−279	2.003
Rb	0.210		1		x	−279	2.003
Sb	0.005		3		x	−255	2.006
Cd	0.157		2		x	−213	2.012
Tc	0.430		4		x	−208	2.016

Comparison with data of Ref. [15] for a similar fuel cross section with average burn-up 98 GWd/tM. Assumed valences of the elements in the fuel matrix and separate oxides according to Kleykamp [9,46]. Oxygen potentials for the corresponding Me/MeO mixtures at 1273 K and equivalent O/M of the mixed oxide $U_{0.6}Pu_{0.4}O_{2\pm x}$ according to data of Lindemer and Brynestad [1].

[a] Dissolved in the fuel with valence 4 (Kleykamp [9]).

[b] Fraction dissolved in the fuel: ZrO_2: ⩽ 25 mol%; SrO_2: ⩽ 12 mol% (Kleykamp [46]).

[c] From Fig. 1.

at large oxygen potentials (see former section). In addition, the assumption of a full oxidation of Cs would imply necessarily that the fuel achieved an O/M ratio greater than 2.001 (e.g. at $T > 1100$ K, see Figs. 1 and 4, Section 2). This latter is in contradiction with the result in [15] yielding to an O/M ratio of the fuel below 1.98.

In the present work, a calculation of the O/M ratio for an equivalent LWR-fuel was undertaken according to the method originally proposed by Holleck and Kleykamp [3]. The fuel composition was calculated with the code SCALE [47] for an average burn-up of 97.7 GWd/tM. The code SCALE combines data entries of neutron cross sections provided by the code Origen [48], with data of the core configuration of the reactor in question. This allows assessing more precisely the neutron flux distribution affecting the particular fuel, leading to realistic results of its burn-up and isotopic composition [49]. The data of the power history and the specific reactor type were taken from [15]. In Table 1 the resulting isotopic composition of the fuel as expected after 4 years decay after extraction is given in weight and atomic concentrations per initial heavy metal atom. The resulting partition of actinides and oxide forming elements, as well as the assumable valence of these elements in the fuel matrix and separate oxides [3,9,46] and the corresponding threshold oxygen potential for their oxidation, are also given in Table 2. The values in Table 2 are compared with compositional values arising from Ref. [15]. The most noticeable differences with Ref. [15] are the yields of the element Mo, here appearing much larger, and those of yttrium and the rare earths elements (Y + RE), here appearing lower than in [15] (Table 2).

Table 3 shows the results of the above mentioned O/M-calculations assuming three different values for the starting fuel stoichiometry (1.995, 2.000 and 2.005) and three oxidation fractions of Mo (100%, 60% and 50%), at a fuel temperature of 1273 K. As mentioned in the introduction, the oxidation of the fuel with progressing burn-up arises from the difference between the roughly 20 oxygen atoms liberated from the fuel every 10 fissions and the roughly 15.6 oxygen atoms needed for the oxidation of the elements Zr, Y + RE and Sr + Ba (LWR-conditions) (Tables 2 and 3). Depending on the initial stoichiometry of the fuel, the oxygen excess is first consumed in the surplus oxidation of the fuel, and further on in the oxidation of the elements Mo, Sn, Cs + Rb, Sb, Cd and Tc, in this order according to the increasing oxygen potentials needed for the formation of their oxides, and the implied increase of oxygen stoichiometry of the fuel (Fig. 1). The corresponding O/M ratios were assigned in Table 3 on the basis of data of the system $U_{0.6}Pu_{0.4}O_{2\pm x}$, which was assumed to well represent the fuel at this burn-up (Fig. 1, Section 2).

The oxygen stoichiometry of the fuel after each oxidation step in Table 3 is governed by the reaction

$$100MO_{(O/M)i} \rightarrow 90MO_{(O/M)i} + (0.25N_{Zr} + 0.12N_{Sr} + N_{Y+RE})O_{(O/M)i} + N_O^{surplus\text{-}fuel} \quad (3)$$

where the final oxygen to metal ratio is expressed by

$$(O/M)_f = (O/M)_i + \frac{N_O^{surplus\text{-}fuel}}{(90 + 0.25N_{Zr} + 0.12N_{Sr} + N_{Y+RE})} = (O/M)_i + \frac{N_O^{surplus\text{-}fuel}}{95.48} \quad (4)$$

where N_{Zr}, N_{Sr} and N_{Y+RE} are the number of atoms of Zr, Sr and Y + RE incorporated to the fuel matrix every 10 fissions and $N_O^{surplus-fuel}$ is the number of extra oxygen atoms

Table 3
Oxygen balance calculation for a LWR-fuel with 98 GWd/tM average pellet burn-up according to method of Holleck and Kleykamp [3]

Initial O/M	Number of oxygen atoms liberated[a]	Oxygen atoms consumed in the oxidation of[a]:													Final O/M
		Zr Y + RE Sr + Ba O/M[b] ≪ 1.99	Fuel	Mo O/M[b] ≅ 2.0003	Fuel	Sn O/M[b] ≅2.0008	Fuel	Cs + Rb O/M[b] ≅ 2.003	Fuel	Sb O/M[b] ≅ 2.006	Fuel	Cd O/M[b] ≅ 2.012	Fuel	Tc O/M[b] ≅ 2.016	
100% oxidation of Mo															
1.995	19.95	15.66	0.51	3.78											2.0003
2.000	20.00	15.66	0.03	4.31											2.0003
2.005	20.05	15.66	–	4.39											2.0003
60% oxidation of Mo															
1.995	19.95	15.66	0.51	2.75	0.05	0.08	0.21	0.670	0.028						2.0033
2.000	20.00	15.66	0.03	2.75	0.05	0.08	0.21	0.670	0.286	0.0075	0.262				2.0087
2.005	20.05	15.66	–	2.75	0.05	0.08	0.21	0.670	0.286	0.0075	0.340				2.0096
50% oxidation of Mo															
1.995	19.95	15.66	0.51	2.29	0.05	0.08	0.21	0.670	0.286	0.0075	0.192				2.0080
2.000	20.00	15.66	0.03	2.29	0.05	0.08	0.21	0.670	0.286	0.0075	0.573	0.157			2.0120
2.005	20.05	15.66	–	2.29	0.05	0.08	0.21	0.670	0.286	0.0075	0.573	0.157	0.068		2.0127

Number of oxygen atoms demanded for 100% oxidation of the element according to Table 2[a]: (Zr, Y + RE, Sr, Ba): 15.66, Mo: 4.58, Sn: 0.08, Cs: 0.565, Rb: 0.105, Sb: 0.0075, Cd: 0.157, Tc: 0.86.

[a] Every 10 fissions.

[b] O/M ratio of the fuel at the oxygen potential of the corresponding Me/MeO mixture at 1273 K (Table 2, Fig. 1).

incorporated in the fuel after oxidation of Zr, Y + Re and Sr + Ba, in first place, and of Mo, Sn, Cs+Rb, Sb, Cd and Tc, in later steps. In the above expressions it is implicit that 25% of Zr and 12% of Sr are dissolved in the fuel matrix. The oxygen consumption after oxidation of the first group of elements (Zr, Y + RE, Sr + Ba), considering an incorporation of 12% of Sr as SrO_2 in the fuel [46], yields 15.66 atoms every 10 fissions (Tables 2 and 3). Analogous numbers were derived in Ref. [3] after 10 at.% burn-up; the O/M ratio after each oxidation step in the fuel was calculated as $(O/M)_f = (O/M)_i + N_O^{surplus-fuel}/90$; the consumption of oxygen in the oxidation of (Zr, Y + RE, Sr + Ba) yielded 14.74 atoms every 10 fissions [3].

In agreement with Ref. [3], Table 3 shows that for a LWR-fuel with an initial O/M ratio between 1.995 and 2.005, all the oxygen excess produced during irradiation up to a burn-up of roughly 100 GWd/tM might be consumed in the oxidation of Mo. Under these conditions the fuel remains at nearly the exact stoichiometry (O/M = 2.0003). Further oxidation of the fuel, so as to achieve values of the oxygen potential allowing the oxidation of, e.g. the fission product Cs, as assumed in [15], would be impossible under these conditions. Only the stagnation of the oxidation of Mo, as eventually derived from the descriptions in Section 3, would allow the occurrence of higher oxygen potentials and higher O/M ratios in the fuel (Table 3). In the examples considered in Table 3, it is shown that such oxidation stagnation at fractions of 50–60% of the available amount of Mo would enable final O/M ratios of the fuel of approximately 2.01–2.013 to be achieved. This agrees well with the oxygen stoichiometry shift previously calculated by Kleykamp [10], i.e., at a rate of $\Delta(O/M) = +0.0013$ per% burn-up (Section 1). The above considerations hold, however, only in the absence of any internal oxidation of the Zr-alloy-cladding.

5. Estimation of the O/M ratio from the lattice parameter variation

Although attempts have been made in the past to estimate the shift of the O/M ratio of the fuel during irradiation on the basis of lattice parameter changes (see Refs. [50–52] for the case of FBR-fuels), the utilisation of this method for high burn-up LWR-fuels had been more recently questioned [14], because of the inherent difficulty to precisely assess the various contributions to this quantity. As mentioned frequently in the literature [12,51,53–55] the lattice spacing of the UO_2 matrix is influenced by a number of processes. It decreases with burn-up, with the incorporation of Pu and with the increase of the O/M ratio. On the other hand, it increases by accumulation of radiation- and α-decay damage, the last particularly during fuel storage after discharge, until a given saturation level is reached [51,55,56]. The release of these internal strains by thermal or a-thermal processes, as, e.g. with the start of the RIM-transformation, causes renewed contraction of the lattice [55].

Despite these influences, in the recent work of Ref. [15] an estimation of the O/U ratio of the already cited LWR-fuel with 100 GWd/tM average burn-up was undertaken on the basis of existing lattice parameter data as a function of the fuel radius, as from measurements reported in [57]. After applying several corrections to the raw data, the authors of [15] concluded that the final O/U ratio of the fuel varied between 1.994 at the centre and 1.961 at the periphery ($r/r_o = 0.99$). The corresponding $O/M^{(*)}$ ratios are, respectively, 1.813 and 1.783 ($^{(*)}O/M = O/U + FP = O/U \times (1 + FP/U)^{-1}$, FP = fission products and actinides atom fractions incorporated to the UO_2 lattice after U-fission, $FP/U \cong 0.1$ at a burn-up of roughly 100 GWd/tM (see Tables 1 and 2)). These very low O/M ratios, not at all harmonizing with the relatively high ΔGO_2-values measured in the same work [15] by the EMF-technique, which even suggest slightly hyperstoichiometric O/M ratios (Section 2), are thought to be caused by imprecision of the method applied.

In [15], the lattice parameter of the fuel was assumed to be that of UO_2 with decreasing Vegard's law contributions from incorporated Pu and single fission products oxides with burn-up (assumption: ideal solutions of UO_2, PuO_2 and fission product oxides of the type MeO_2, as from Benedict et al. [51]), plus an increasing contribution due to α-damage during storage, assumed to be proportional to the Pu concentration. An ad hoc correction for accumulated lattice strains during irradiation was also undertaken across the fuel radius. After addition/subtraction of the estimated quantities, the corrected values were postulated to fit in the line 'lattice constant vs. O/U', which was assumed to be valid up to O/U = 1.96 [15]. This despite the homogeneity range of hypostoichiometric UO_2 is proven to be almost inexistent at temperatures below 1300 K (see reviewed UO_2 phase diagram in [24]). As a result, the derived (corrected) lattice constant values, which varied roughly between 547.2 and 547.6 pm (see Fig. 7a in Ref. [15]), i.e., quite above that of stoichiometric UO_2 (547.02 pm), were assigned by extrapolation to correspond to O/U ratios decidedly below 2 (see Fig. 7b in Ref. [15]).

As a complement of the above, Fig. 7 shows a review of the lattice constant of uranium oxide as a function of the O/U ratio in the range UO_2–U_4O_9, based on the early data by Swanson and Fuyat [58], Grønvold [59] (only for stoichiometric UO_2), Shaner [60], Hoekstra [61] and Lynds et al. [62], and more recent data from Lucuta et al. [63]. In the range $2 \leqslant O/U \leqslant 2.125$ the values appear quite scattered; the lower bound is constituted by those of Lynds et al. [62], which follow a well defined slope (Fig. 7). Out of this range fall the estimations by Javed [64] (Fig. 7), who calculated the lattice parameter of UO_{2+x} using the data of Grønvold [59], i.e., assuming mixtures of UO_2 and U_4O_{9-y} (Grønvold's samples were not single-phase at room temperature [59]). For the range UO_{2-x}, whose composition limit is shown in Fig. 7 according to [24], Javed [64] pointed out that the lattice constant is essentially the same as for stoichiometric UO_2 (sic). The interpolation

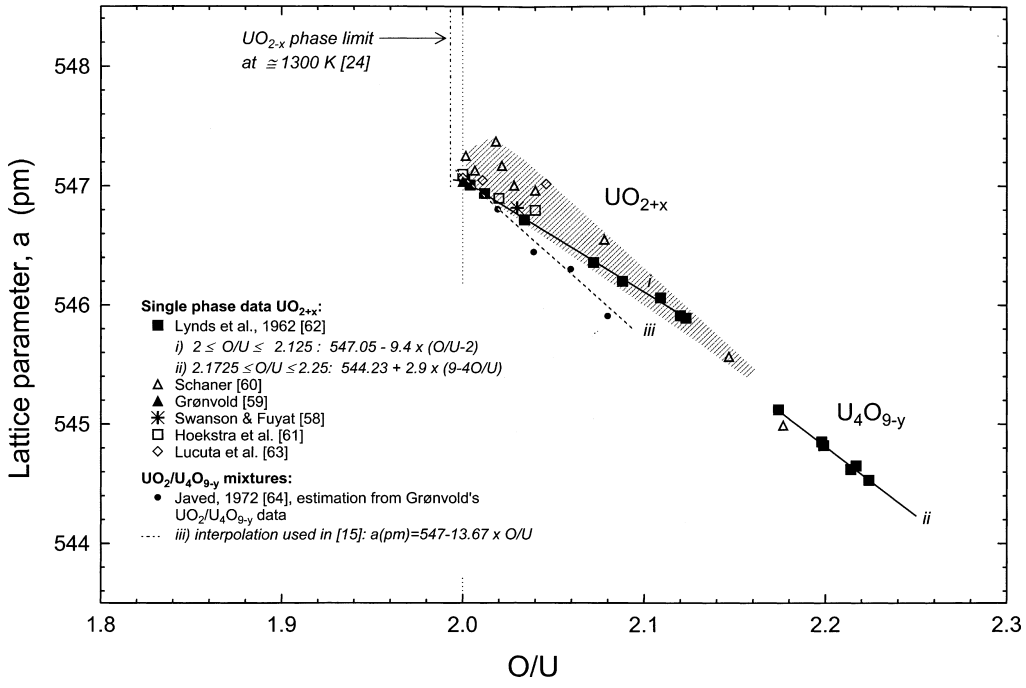

Fig. 7. Lattice constant vs. O/U ratio data for uranium dioxide in the phase-field ranges UO_{2+x} and U_4O_{9-y}.

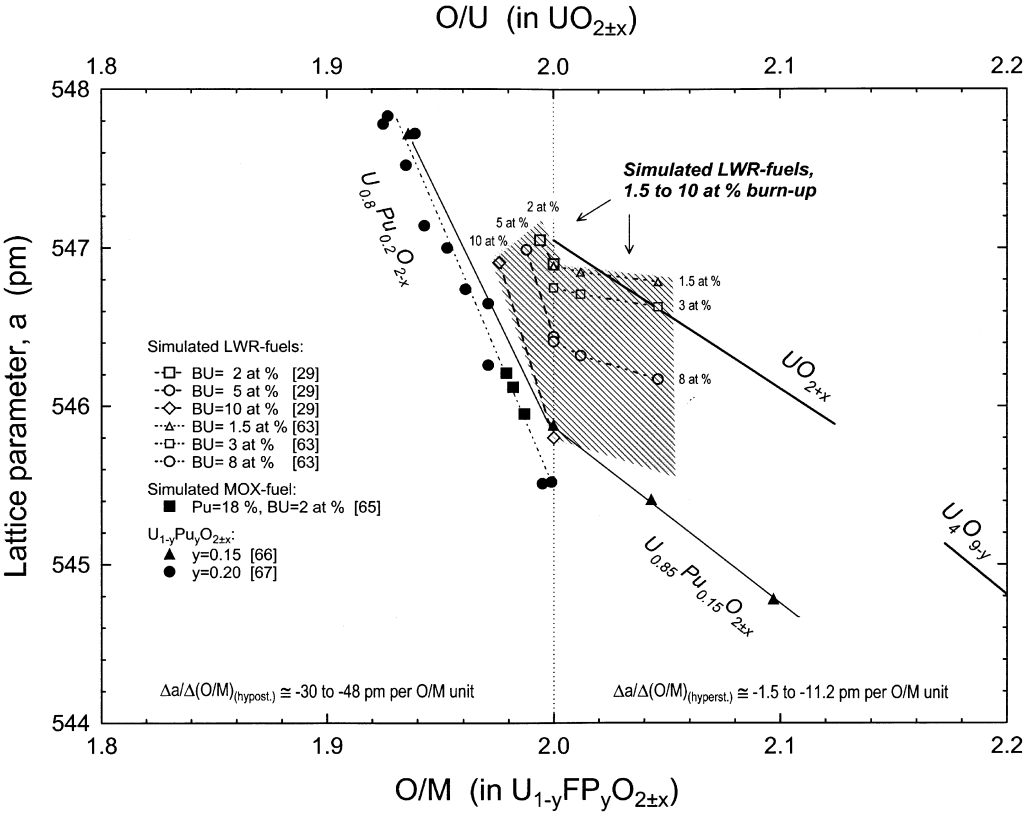

Fig. 8. Lattice constant vs. O/M ratio data for simulated spent LWR and MOX-fuels and the systems $U_{1-y}Pu_yO_{2\pm x}$ ($y = 0.15$, 0.20). Comparison with data of uranium dioxide as from Fig. 7.

of Grønvold's hyperstoichiometric data, as undertaken in [64] and as also used in [15] (Fig. 7), is therefore approximate, and only valid for the range $O/U \geqslant 2$.

Fig. 8 shows in addition the available literature data of lattice constant vs. the O/M ratio for simulated LWR [29,63]- and MOX [65]-fuels and two $U_{1-y}Pu_yO_{2\pm x}$ systems

($y = 0.15$ [66], $y = 0.2$ [67]), as compared to the previously described boundary for UO_{2+x} and U_4O_{9-y} according to Lynds et al. [62] (Fig. 7). As already mentioned in Section 2.1 concerning the ΔGO_2 vs. O/M data, it is seen in Fig. 8 that the addition of Pu and/or fission products to the UO_2 lattice opens the hypostoichiometric field (homogeneity range) of the respective systems. However, it is to be observed that the influence of the O/M ratio in the lattice constant of the mixed oxides is quite different at both sides of the exact stoichiometry, i.e., it is about 3 to 4 times stronger in the hypostoichiometric as in the hyperstoichiometric range ($\Delta a/\Delta(O/M)_{(hypost.)} \cong -30$ to -48 pm per O/M unit; $\Delta a/\Delta(O/M)_{(hyperst.)} \cong -1.5$ to -11.2 pm per O/M unit) (Fig. 8). Similar trends are confirmed for a variety of U–Me–O systems (see corresponding review in Ref. [23]). The extrapolation of behaviours from one range into the other is therefore not valid. In addition, it is seen that as for the simulated fuels [29,63], the influence of the O/M ratio in the lattice constant seems to be the larger, the higher the burn-up is (Fig. 8).

Fig. 9 shows in another form how the influences of burn-up and the O/M ratio in the lattice parameter of the fuel are interrelated. Here the lattice parameter of irradiated and simulated LWR-fuels from different sources (respectively, [4,56,68] and [29,40]) are plotted as a function of burn-up, after heat treatments were made at different oxygen potentials (Fig. 9). Although only a qualitative comparison of these data can be made because of the different temperatures involved, it is seen that in general the influence of burn-up on the lattice constant is the larger, the higher the oxygen potential (O/M ratio) is (Fig. 9). In the burn-up range of our interest (BU $\leqslant$ 100 GWd/tM), the data of Une and Oguma [29] show that for the stoichiometric fuel (O/M $\cong 2$, $T = 1273$ K, $\Delta GO_2 = -380$ kJ/mol), the decrease of the lattice constant with burn-up occurs with a slope of approximately -0.129 pm per 10 GWd/tM (Fig. 9). For higher oxygen stoichiometry of the fuel, higher decreasing slopes are expected, and vice versa.

The above shows the difficulties of an assessment of the O/M ratio of the irradiated fuel based on the lattice constant, apart from the not fully certain shift of the data due to radiation and α-decay damage. A qualitative estimation of the trends can be attempted, however, from the comparison of the lattice constant profiles vs. the pellet radius for different fuels. Such a comparison is made in Fig. 10 for the irradiated LWR-fuels with average burn-ups of 67, 80 and 98 GWd/tM, as from data reported in [55,57]. The reduction in the lattice constant towards the centre and the periphery of the fuels are attributed according to [55] to the thermal and a-thermal (RIM transformation-triggered) release of lattice strains. At the onset of the RIM-zone, where the local burn-up nears the average burn-up, the impact of the lattice damage is maximum. As this influence seems to reach saturation for local burn-ups above 60–70 GWd/tM [55], the change of the

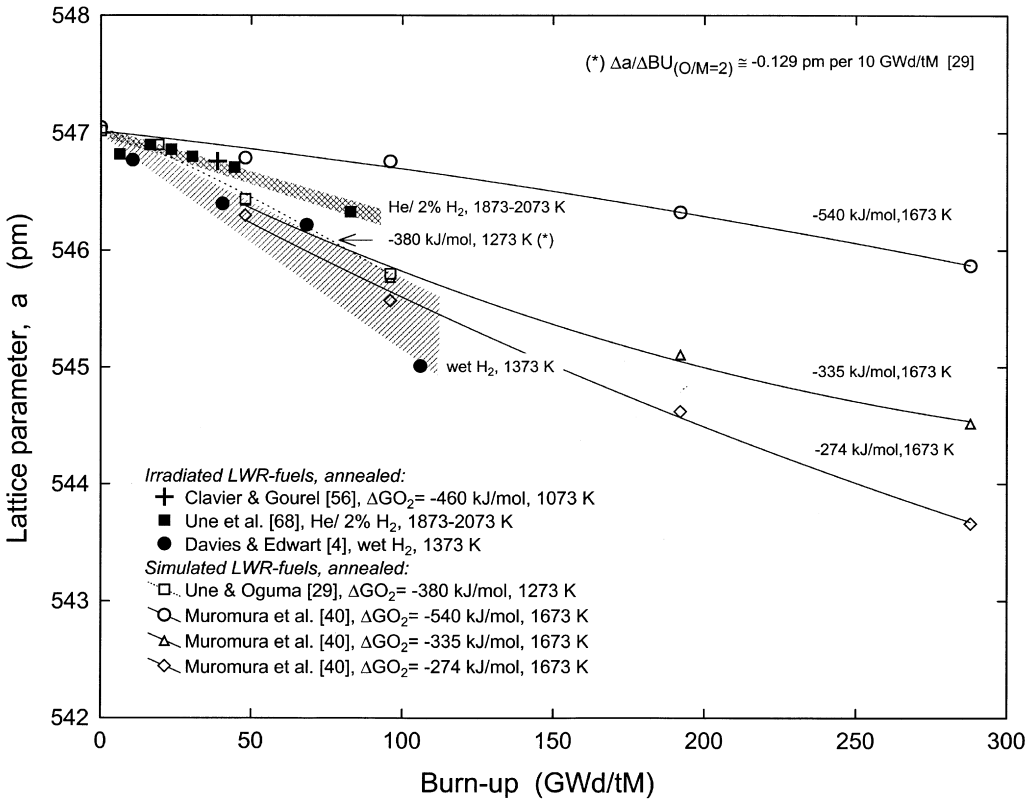

Fig. 9. Lattice constant vs. burn-up data for irradiated and simulated LWR-fuels after annealing at different oxygen potentials and temperature.

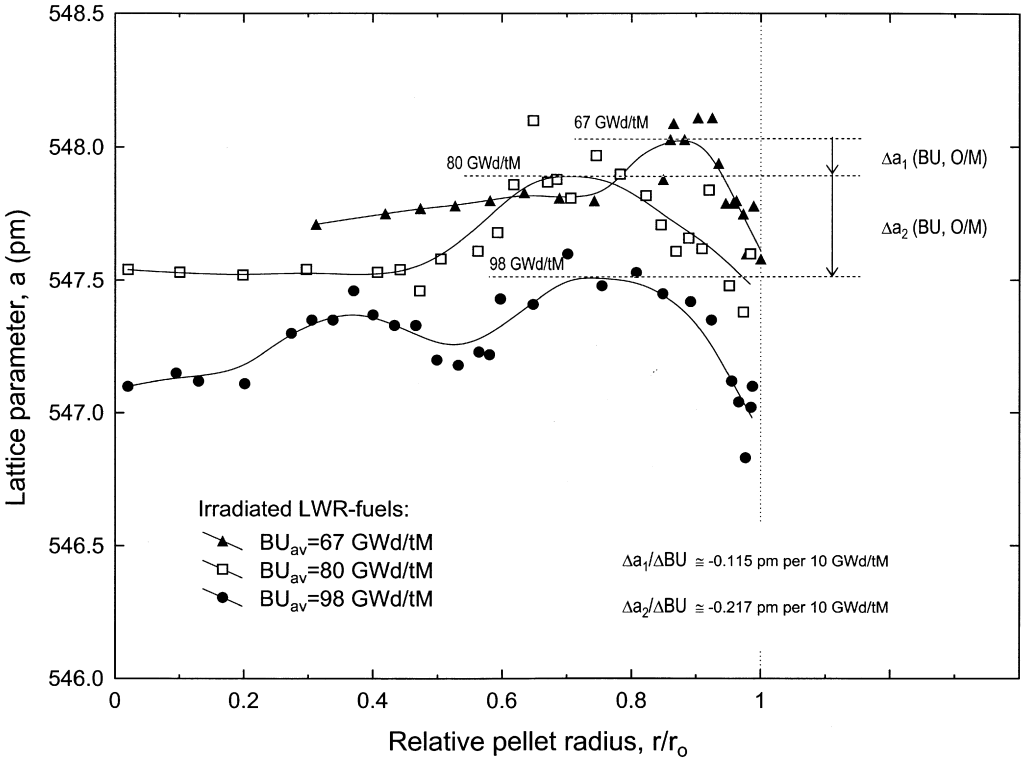

Fig. 10. Lattice constant vs. radial position data for irradiated LWR-fuels with average burn-ups 67, 80 and 98 GWd/tM, as from micro XRD measurements previously reported in Refs. [55,57].

lattice parameter at this position between different fuels would follow differences in the local burn-ups and the local O/M ratios. Fig. 10 shows that the slope of this change for the fuels with average burn-ups between 67 and 80 GWd/tM (−0.115 pm per 10 GWd/tM) is close to the above quoted value for stoichiometric fuels (Fig. 9). In turn, the equivalent slope for the fuels with average burn-ups between 80 and 98 GWd/tM (−0.217 pm per 10 GWd/tM) (Fig. 10), suggests that the higher burn-up fuel is to be in the hyperstoichiometric range (Fig. 9), at least for the radial position considered. This is in line with the conclusions of Section 2.

6. Discussion

Throughout the different sections of the present work it has been shown unambiguously that LWR-fuels irradiated up to very high average burn-ups, say beyond 80 GWd/tM and especially beyond 100 GWd/tM, are most likely to become hyperstoichiometric during the last irradiation cycles. This trend resulted unmistakably from the comparison of measured ΔGO_2 values by the EFM-method with available thermodynamic data of simulated LWR-fuels and the reference system $U_{0.4}Pu_{0.6}O_{2\pm x}$, which is shown to reasonably represent the behaviour of the high burn-up fuel (Section 2). The same was supported also qualitatively in accompanied fuel composition calculations (Section 4) and lattice parameter profiles analysis (Section 5).

The above results stay in contradiction with the recent prediction by Walker et al. [15] of their examined LWR-fuel with average burn-up 100 GWd/tM to acquire a definite hypostoichiometric oxygen composition despite the high ΔGO_2 values measured (Figs. 2 and 4). The discrepancy is attributed to imprecision of the methods applied in [15] to derive the O/M ratios both from fuel composition calculations and from lattice constant data (Sections 4 and 5). In turn, for lower average extraction burn-ups, say below 80 GWd/tM, the present analysis fully agree with the previous predictions by Kleykamp [10] and Matzke [13,14] indicating the irradiated LWR-fuels to remain roughly stoichiometric or slightly hypostoichiometric, this last particularly near the pellet edge. The O/M ratios in these cases are shown to oscillate between 2 and a value not inferior to 1.999 (Fig. 4).

Although slight, the expected oxidation of the fuel at very high burn-ups, with possible final O/M ratios ranging between 2.001 and 2.002 (Figs. 2 and 4), may cause a measurable increase of the diffusivity of species (e.g., U, Xe) in the matrix, and a tangible increase of the fission gas release fraction. As for the self-diffusion coefficient of uranium in UO_{2+x} (the same argument applies to the creep rate), measurements by Matzke [69] and Marin and Contamin [70] showed this to increase in the temperature range 1200–1650 °C proportionally to $x^{1.5}$ [69] or x^2 [70]; $x(>0)$ is the departure from the exact stoichiometry. A similar increase with the stoichiometry shift was also found for the diffusion coefficient of Xe in UO_{2+x} in the early work by Lindemer

and Matzke [71]. Although contradictory results by Miekeley Felix [72] appeared later and controversies were raised concerning the stoichiometry state and the diffusion models applicable [73], the consensus was established that the slightest increase in the oxygen content will cause dramatic increase of the release rates of the rare gases in UO_2 (sic) [74]. As reviewed by Mansouri and Olander [75] the diffusivity of Xe in the fuels was thus described to vary proportional to $x^{1.3}$, as for the data of [71], or to x^2, as for newer irradiation data and mechanistic model by Killeen and Turnbull [76]. This implies an increase of about 20–100 times for a change of x between, e.g. 0.0001 and 0.001.

As for the fractional release of Xe from UO_{2+x} in annealing tests, experiments at 1000 °C in both Ref. [71] and the later work by Shiba [77] coincide well showing a monotonic increase of the released fraction (F) with the stoichiometry shift (x) ($F \propto (Dt)^{1/2}$, D = effective diffusion coefficient, t = annealing time [75]); with F increasing from values of less than 1% at $x \cong 0$, to values close to 10% at $x \cong 0.2$ [73]. According to the recent study by Kim [78] of fission gas release in defective LWR-fuels, the data of Shiba [77] can be well fitted by an expression of the type $F = 0.007 + 0.6x - 1.1x^2$. This implies F increasing by about 17%, for x changing from zero to a value of about 0.002.

Whether the described increase of the O/M ratio of these fuels at very high burn-ups may have had a measurable impact in their gas release fractions would be dependent of the power history, and of the time at which the O/M shift entered in play. This assessment is beyond the scope of the present work. The purpose of the authors at this point is just to remark that due to this influence, regions of the fuel otherwise excluded from gas release by thermal reasons, particularly those adjacent to the depleted centre, may potentially enter in play. This in connection, it seems worthy to recall the works by Une and co-workers [54,79] about fission gas release from defective-oxidised BWR fuels. In these works, it has been shown that after fuel oxidation by water vapour entrance after the failure, the limit of the inner fuel region depleted in Xe increased from roughly $r/r_o \cong 0.55$ in the sound fuel, to $r/r_o \cong 0.75$ in the defective fuel [79], with r/r_o = relative pellet radius. The levels of oxidation of the defective fuels were, however, remarkably higher than the considered for the fuels of this paper (in [79]: $(O/M)_{final} \cong 2.02$–2.05).

Regarding the causes for the anticipated slight fuel oxidation at very high burn-ups, only the stagnation of the oxygen uptake by the cladding, and the stagnation of the oxidation of the fission product Mo (Sections 3 and 4) can be mentioned as possible. Fig. 11 shows that the thickness (10–15 μm) and aspect of the fuel-cladding interaction oxide layer of the studied LWR-fuels remained almost unchanged between approximately the 6th and the 9th irradiation cycle (67 to 98 GWd/tM). It is thus possible that the overall oxygen up-take by the cladding became saturated around the 6th cycle and above. To the knowledge of the authors, measurements of the oxygen concentration profile at the inner side of the cladding at these high burn-ups are not available. As for the role of Mo, Section 4 shows that only a stagnation of its oxidation at a level of highest 80% of the inventory may allow the O/M ratio of the fuel to reach the mark of ≅2.002. At this oxygen content in the fuel, the oxidation of Cs, otherwise assumed to be 100% in [15], may be also excluded (Sections 3 and 4).

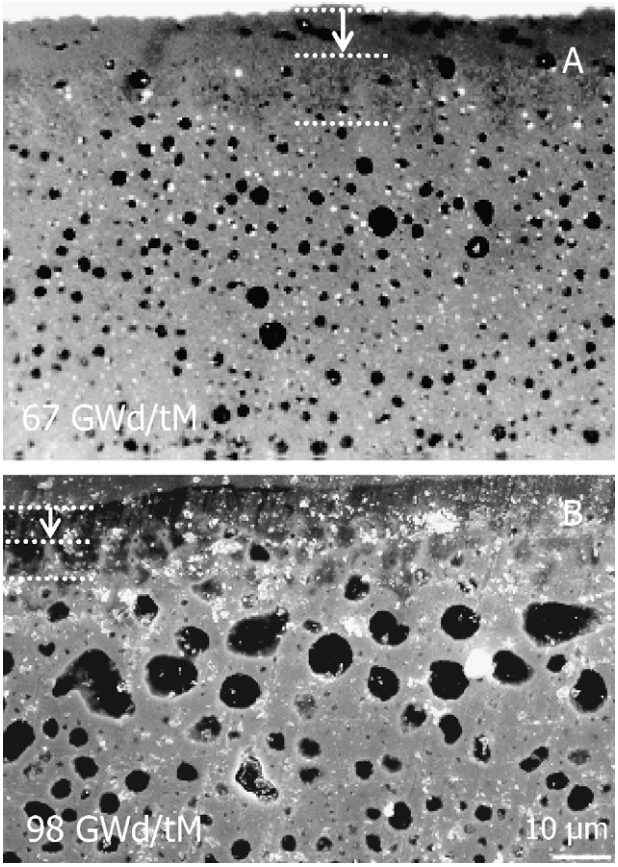

Fig. 11. Fuel-cladding interaction layers in two irradiated LWR-fuels with average burn-ups 67 GWd/tM (A) and 98 GWd/tM (B). Two interaction layers are visible: a continuous one attached to the cladding and a discontinuous one penetrating the fuel. The thickness and the aspect of both types of oxide layers appear similar at the two burn-ups. (A) and (B) show same magnification.

The present review has shown how crucial is the availability of thermodynamic data of the irradiated or simulated fuels, in order to assess the oxygen balance at high burn-up and its potential impact on important properties like gas release. Determination of the O/M ratio in the fuel by alternative methods like composition calculations or derivations from lattice constant values may be useful for a qualitative approach, but eventually subjected to error, as in the case of the lattice constant being influenced by various parameters with interrelated effects. Important for this purpose is the availability of reliable data of the quantity ΔGO_2 as a function of temperature and of the real measured fuel matrix composition (O/M, U/U + FP ratios); as well as of data of the accompanied modifications of the metallic and oxide precipitates compositions under

variations of the oxygen potential and temperature. In this aspect, if a more substantiated assessment of the modification of the oxygen balance of LWR-fuels under irradiation is needed, particularly in view of their potential insertion at average burn-ups beyond 70 GWd/tM, more detailed experimental studies in the referred areas are necessary.

As a complement, the independent determination of the O/M ratios in the fuel by chemical methods may be considered as an option to the otherwise troublesome thermogravimetric method for irradiated fuels due to the evaporation of volatile species. In this respect, the modified spectrophotometric method by Kihara et al. [19], which has been frequently utilized for U–Me–O systems [18], and other chemical methods likewise based in the determination of the U^{4+}/U^{6+} ratio in solution (e.g. flow coulometry, polarography), as those early used for UO_{2+x} [62] and already put in practice for low burn-up irradiated LWR-fuels [20,21], may be worthwhile to be explored for the high burn-up fuels.

7. Conclusions

The available oxygen potential (ΔGO_2) data of LWR-fuels by the EFM-method have been reviewed and compared with thermodynamic data of equivalent simulated fuels and mixed oxide systems, accompanied by qualitative estimation of the oxygen stoichiometry (O/M) trends by fuel composition calculations and lattice constant analysis.

The comparison confirmed previous predictions by Kleykamp [10] and Matzke [13,14] indicating LWR-fuels to remain stoichiometric or slightly hypostoichiometric, the last basically at the interface with the cladding, up to average burn-ups in the range 70–80 GWd/tM. Recent predictions of a highly exposed fuel with average burn-up around 100 GWd/tM to become decidedly hypostoichiometric were not confirmed. In turn, the analysis of data shows that approximately at burn-ups around 80 GWd/tM and above, the fuels tend to become progressively slightly hyperstoichiometric; the maximum O/M ratios potentially achieved at an average burn-up of 100 GWd/tM would range between 2.001 and 2.002. The causes for this hyperstoichiometric shift are attributed to the stagnation of the oxygen up-take by the cladding and certain stagnation in the oxidation of the fission product Mo. The foreseen slight increase of the oxygen content of the fuel matrix may have, however, an accelerating impact in the fission gas release rates. The magnitude of this last would depend on the power history and of the stage at which the positive O/M-ratio-shift enters in play.

References

[1] T.B. Lindemer, J. Brynestad, J. Am. Ceram. Soc. 69 (1986) 867.
[2] D.R. O'Boyle, F.L. Brown, J.E. Sanecki, J. Nucl. Mater. 29 (1969) 27.
[3] H. Holleck, H. Kleykamp, Report KfK 1181, August 1970.
[4] J.H. Davies, F.T. Ewart, J. Nucl. Mater. 41 (1971) 143.
[5] J.R. Finlay, in: Proceedings of a Panel on the Behaviour and Chemical State of Irradiated Ceramic Fuels, IAEA, 7–11 August 1972. STI/PUB/303, Panel Proceedings Series, IAEA, Vienna, 1974, p. 31.
[6] D.R. Olander, TID-26711-P1, 1976.
[7] I. Barin, Thermochemical Data of Pure Substances, third edition in collaboration with G. Platzki, vols. I–II, VCH, Weinheim, Germany, 1995. ISBN 3-527-28745-0.
[8] O. Knacke, O. Kubaschewski, K. Hesselmann (Eds.), second ed., Thermochemical Properties of Inorganic Substances, vols. I–II, Springer-Verlag, 1991.
[9] H. Kleykamp, J. Nucl. Mater. 131 (1985) 221.
[10] H. Kleykamp, J. Nucl. Mater. 84 (1979) 109.
[11] M.G. Adamson, E.A. Aitken, S.K. Evans, J.H. Davies, Thermodynamic of Nuclear Materials, IAEA-SM-190/54, Vienna, 1974, vol. I, p. 59.
[12] K. Une, Y. Tominaga, S. Kashibe, J. Nucl. Sci. Technol. 28 (1991) 409.
[13] Hj. Matzke, J. Nucl. Mater. 208 (1994) 18.
[14] Hj. Matzke, J. Nucl. Mater. 223 (1995) 1.
[15] C. Walker, V. Rondinella, D. Papaioannou, S. Van Winckel, W. Goll, R. Manzel, J. Nucl. Mater. 345 (2005) 192.
[16] Y. Saito, J. Nucl. Mater. 51 (1974) 112.
[17] K. Une, M. Oguma, J. Nucl. Mater. 110 (1982) 215.
[18] K. Une, M. Oguma, J. Nucl. Mater. 115 (1983) 84.
[19] S. Kihara, T. Adachi, H. Hashitani, Fresenius Z. Anal. Chem. 303 (1980) 28.
[20] H. Takeishi, H. Muto, H. Aoyagi, T. Adachi, K. Izawa, Z. Yoshida, H. Kawamura, S. Kihara, Anal. Chem. 58 (1986) 458.
[21] S.R. Sarkar, K. Une, Y. Tominaga, J. Radioanal. Nucl. Chem. 220 (1997) 155.
[22] T. Lindemer, T. Besmann, J. Nucl. Mater. 130 (1985) 473.
[23] T. Fujino, C. Miyake, in: A.J. Freeman, C. Keller (Eds.), Chapter 3 in Handbook on the Physics and Chemistry of the Actinides, Elsevier Science Publishers B.V., 1991, p. 155.
[24] (a) M. Baichi, C. Chatillon, G. Ducros, K. Froment, J. Nucl. Mater. 349 (2006) 17;
(b) M. Baichi, C. Chatillon, G. Ducros, K. Froment, J. Nucl. Mater. 349 (2006) 57.
[25] T. Besmann, T. Lindemer, J. Nucl. Mater. 130 (1985) 489.
[26] T. Besmann, T. Lindemer, J. Nucl. Mater. 137 (1986) 292.
[27] T.B. Lindemer, A. Sutton, J. Am. Ceram. Soc. 71 (1988) 553.
[28] K. Une, M. Oguma, J. Nucl. Mater. 118 (1983) 189.
[29] K. Une, M. Oguma, J. Nucl. Sci. Tech. 20 (1983) 844.
[30] R.E. Woodley, J. Nucl. Mater. 74 (1978) 290.
[31] P. Gerdanian, M. Dodé, J. Chim. Phys. (1965) 171.
[32] C. Thomas, P. Gerdanian, M. Dodé, J. Chim. Phys. Phys. Chim. Biol. 65 (1968) 1349.
[33] T.L. Markin, R.J. Bones, Report AERE-R4178, November 1962.
[34] V.G. Baranov, Yu.G. Godin, Atom. Energy (Translation) 51 (1981) 228.
[35] H. Kleykamp, J. Nucl. Mater. 66 (1977) 292.
[36] H. Kleykamp, J.O. Paschoal, R. Pejsa, F. Thümmler, J. Nucl. Mater. 130 (1985) 426.
[37] J.O.A. Paschoal, PhD Dissertation, Univ. Karlsruhe, Report KfK 3473, 1983.
[38] J.O.A. Paschoal, H. Kleykamp, F. Thümmler, Z. Metallkde. 74 (1983) 652.
[39] J.O.A. Paschoal, H. Kleykamp, F. Thümmler, J. Nucl. Mater. 151 (1987) 10.
[40] T. Muromura, T. Adachi, H. Takeishi, Z. Yoshida, T. Yamamoto, K. Ueno, J. Nucl. Mater. 151 (1988) 318.
[41] T. Adachi, T. Muromura, H. Takeishi, T. Yamamoto, J. Nucl. Mater. 160 (1988) 81.
[42] S. Imoto, J. Nucl. Mater. 140 (1986) 19.
[43] H. Kleykamp, J. Nucl. Mater. 171 (1990) 181.
[44] H. Kleykamp, Nucl. Tech. 80 (1988) 412.
[45] P.G. Lucuta, R.A. Verall, Hj. Matzke, B.J. Palmer, J. Nucl. Mater. 178 (1991) 48.
[46] H. Kleykamp, J. Nucl. Mater. 206 (1993) 82.

[47] SCALE 4.3: Modular code system for performing Standardised Computer Analysis for Licensing Evaluation, RSIC-CCC-545, ORNL.
[48] A.G. Croff, Origen 2, A revised and up-dated version of the Oak Ridge Isotope Generation and Depletion Code, Report ORNL-5621 UC-70, 1980.
[49] M. Wallenius, P. Peerani, L. Koch, J. Rad. Nucl. Chem. 246 (2000) 317.
[50] F. Schmitz, G. Dean, M. Halachmy, J. Nucl. Mater. 40 (1971).
[51] U. Benedict, M. Coquerelle, J. De Bueger, C. Dufour, J. Nucl. Mater. 45 (1972/1973) 217.
[52] H. Kleykamp, R. Pejsa, J. Nucl. Mater. 124 (1984) 56.
[53] K. Nogita, K. Une, J. Nucl. Sci. Technol. 30 (1993) 56.
[54] K. Une, M. Imamura, M. Amaya, Y. Korei, J. Nucl. Mater. 223 (1995) 40.
[55] J. Spino, D. Papaioannou, J. Nucl. Mater. 281 (2000) 146.
[56] B. Clavier, Y. Gourel, Measures du paramètre cristallins des crayons Gravelines et Saint-Laurent B1 par diffraction des rayons X. CEA, DRN, Report DMT-94/07/SETIC/LECR-94/01, 1994.
[57] J. Spino, Safety of Nuclear Fuels: High Burn-up Fuel Performance, The European Commission, Institute for Transuranium Elements, Germany, 2001, p. 54 (Report Eur 20252 EN).
[58] H.E. Swanson, R.K. Fuyat. Standard X- Ray Diffraction Powder Patterns, National Bureau of Standards Circular 539, vol. II, Washington, 1953.
[59] F. Grønvold, J. Inorg. Nucl. Chem. 1 (1955) 357.
[60] B.E. Schaner, J. Nucl. Mater. 2 (1960) 110.
[61] H.R. Hoekstra, A. Santoro, S. Siegel, J. Inorg. Nucl. Chem. 18 (1961) 166.
[62] L. Lynds, W.A. Young, J.S. Mohl, G.G. Libowitz, in: Nonstoichiometric CompoundsAdvances in Chemistry Series, vol. 39, American Chemical Society, Washington, DC, 1963, p. 58.
[63] P.G. Lucuta, R.A. Verrall, Hj. Matzke, I.J. Hastings, in: Third International Conference on CANDU Fuel, Chalk River, Canada, October 4–8, 1992, p. 2.
[64] N.A. Javed, J. Nucl. Mater. 43 (1972) 219.
[65] F. Schmitz, in: International Nuclear Symposium on American Ceramic Society, Washington, May 1969, p. 32.
[66] T.L. Markin, R.S. Street, J. Inorg. Nucl. Chem. 29 (1967) 2265.
[67] As cited in M.A. Mignanelli, P.E. Potter, J. Less Comm. Met. 121 (1986) 605;
from data sources: G. Dean, as cited in [50].;
A.E. Martin, W.A. Shin, Rep ANL-7877,1972.;
M. TetenbaumProceedings of the Symposium on Thermodynamics of Nuclear Materials, 1974, vol. 2, IAEA, Vienna, 1974, p. 305.
[68] K. Une, K. Nogita, S. Kashibe, M. Imamura, J. Nucl. Mater. 188 (1992) 65.
[69] Hj. Matzke, J. Nucl. Mater. 30 (1969) 26.
[70] J.F. Marin, P. Contamin, J. Nucl. Mater. 30 (1969) 16.
[71] R. Lindner, Hj. Matzke, Z. Naturforsch. 14a (1959) 582.
[72] W. Miekeley, F.W. Felix, J. Nucl. Mater. 42 (1972) 297.
[73] Hj. Matzke, Radiat. Eff. 53 (1980) 219.
[74] G.T. Lawrence, J. Nucl. Mater. 71 (1978) 195.
[75] M.A. Mansouri, D.R. Olander, J. Nucl. Mater. 254 (1998) 22.
[76] J.C. Killeen, J.A. Turnbull, in: Proceedings of the Workshop on Chemical Reactivity of Oxide Fuel and Fission Product Release, Gloucestershire, UK, 1987, p. 387.
[77] K. Shiba, J. Nucl. Mater. 57 (1975) 271.
[78] Y.S. Kim, Fission Gas Release from UO_{2+x} in Defective Light Water Reactor Fuel Rods, Report ANL/EA/CP-100465, 2000.
[79] K. Une, M. Imamura, M. Amaya, Y. Korei, J. Nucl. Mater. 226 (1995) 323.